OXYGEN ATOM VELOCITY DISTRIBUTIONS AS VIEWED FROM A SPACECRAFT AND THEIR USE TO DETERMINE THERMOSPHERIC TEMPERATURES

P. N. Peters, R. C. Sisk, and J. C. Gregory*

Submitted To:

Geophysical Research Letters

SPACE SCIENCE LABORATORY
PREPRINT SERIES
NO. 86-128

May 1986

*Department of Chemistry
The University of Alabama in Huntsville
Huntsville, AL 35899

Abstract. The angular distributions of oxygen atoms incident on surfaces in low Earth orbit have been calculated for a number of ambient atom temperatures. Atom fluxes to surfaces were modeled by integrals over all permitted angles of incidence. Angles of incidence are limited by masking structures and a number of types are described. Combustible surfaces are heavily etched, creating profiles in mask shadows which are sensitive to ambient temperatures. Profiles measured for a September 1983 flight were fit to our model profile with a temperature of 750±50 K, which agrees with estimates based on solar activity at that time.

Introduction

The Maxwell-Boltzmann distribution of speeds of atoms or molecules is asymmetric, but the speeds have random directions so the distribution is spatially symmetric as viewed from a stationary reference frame, and a Gaussian or normal distribution results from examining components parallel to any one axis. However, relative to a rapidly moving spacecraft ($\approx$7.8 km s^{-1} in the thermosphere between 200 and 600 km) the incidence angles of atoms striking surfaces are greatly limited. For forward-facing surfaces the particles are incident within a narrow cone with the flux strongly peaked about normal incidence. The orbital velocity is thus a dominant factor in spaceborne measurements of ambient particles. In this discussion, flux refers to the differential quantity in atoms cm^{-2} s^{-1}, while fluence refers to the flux integrated over time.

Combustible materials, such as carbon and polycarbonate plastics, exhibit heavy etching due to formation of volatile oxides from low activation energy reactions with atomic oxygen in orbit (J. C. Gregory and P. N. Peters, unpublished proposal, 1975) [Gregory and Peters, 1984, 1985; Leger, 1982;

Peters et al., 1983; Visentine et al., 1985]. Studying the effects on surfaces located behind shadowing structures during exposure in orbit provides a means of investigating the thermal speed distribution of oxygen atoms in the thermosphere, as previously noted [Peters et al., 1983].

Modeling the Angular Distribution

Nocilla [1963] has considered the case of a moving ensemble of gas molecules. The angular distribution of a beam of gases scattered from a surface was determined by combining the thermal speeds of the particles with their ensemble velocity. Forward-facing surfaces on an orbiting spacecraft experience the equivalent of a high velocity beam incident on exposed areas. To combine the thermal speeds with the orbital velocity we have adapted Nocilla's method with the modification that gases passed through differential areas rather than scattered from them. An important parameter in the Nocilla model is the ratio of the translational speed of the "mass" (or ensemble) to the most probable speed. Our analogous parameter is the ratio of orbital speed to the most probable speed. We varied this parameter by adjusting the temperature.

Experimental Technique

Since combustible solid surfaces are heavily etched by exposure to atomic oxygen in orbit, if a portion of the sensitive surface is protected by a metal mask, the shape of the edge of the etched area is affected by the angular distribution of the active oxygen atoms striking the surface. On the STS-8 flight of the space shuttle a number of surfaces were exposed to the ambient oxygen in orbit as part of a materials evaluation experiment [Visentine et

al., 1985]. This flight was particularly suited to the experiment discussed here since during the entire mission 95% of the 3.5×10^{20} atoms cm^{-2} fluence was accumulated with the Orbiter pointing the experiments within 1° of the orbital direction. The vitreous carbon disc was mounted on a heated surface which was tilted slightly (~4°) with respect to the velocity direction. The polished carbon surface was mounted behind a solid aluminum mask that had an effective height (thickness) of 560 μm at a hole exposing the carbon. Other combustible samples, such as CR-39 (a polycarbonate plastic), were mounted behind masks with knife edges essentially in contact with the sample surfaces and some samples had thin film mask patterns deposited directly on their surfaces.

Surface profiles of the etched areas where mask edges existed were measured after the flight with a stylus profilometer (Tencor Instrument's Alpha-Step 200). Theoretical etch profiles for several simple physical configurations of mask and surface were deduced from integrals of angular distributions calculated for oxygen atoms striking an etchable surface partially covered by a mask (Figure 1). Comparisons of such theoretical profiles to measured etch profiles were used to estimate the average ambient temperature during exposure.

Results

Computer-generated solutions to Nocilla's equations [Nocilla, 1963] are presented for three speed ratios (Figure 2): zero (the imaginary case of a stationary satellite, or an ensemble of gases moving with the satellite); unity (imaginary case where the most probable thermal speed equals the orbital speed); and 8:1 (a typical case where the orbital speed is eight times the most probable thermal speed). The polar plot emphasizes the "beam" concept,

while rectangular plots and their integrals are more easily applied to effects resulting from atomic oxygen exposure. Since the temperature of the thermosphere is strongly dependent on solar activity, cases for high and low solar activity conditions are shown (Figure 3). It should be noted that, unlike Nocilla, we have normalized the maxima of all distributions to unity, so only percentages of maximum as a function of angle are displayed. This simplifies presentation, since the lobe for the 8:1 ratio (Figure 2), normalized according to total fluence (equal areas for equal fluences), would have a much larger maximum than the others. Also, the maximum etch depths would be greatest for solar maximum conditions that produce the largest densities of ambient oxygen atoms. The cosine distribution (Figure 2) agrees with the limiting case for effusion of gases through an orifice where both the gas ensemble and the orifice are stationary. The progressive elongation of the angular distribution with speed ratio is also consistent with observations. Such angular distributions can be used to visualize the "spread" that particles exhibit after passing through a small area or to describe the angles of incidence on differential areas on forward-facing surfaces.

It is apparent from a rectangular plot of a typical angular distribution (Figure 3) that few atoms strike forward-facing surfaces with angles of incidence exceeding 15° off-normal. In fact, in the wake of a shielding surface with no scattering, the flux of particles beyond 40° behind the edge of the shield is calculated from our distributions to be less than 10^{7} cm^{-2} s^{-1}, which corresponds to less than the flux to surfaces due to a pressure of 10^{-14} torr (average mass 28 amu).

A number of theoretical etch profiles have been examined (Figure 1). For a surface located behind a slit at a distance large compared to the slit width, the etch profile perpendicular to the slit should have the shape of an

inverted angular distribution (Figure 1a). The situation for an elevated half-plane mask is somewhat different (Figure 1b) in that etched areas approaching the edge of the half-plane from the right receive progressively less fluence (more area under the distribution curve is blocked). Vertically under the edge all atoms incident from the left of the edge have been blocked, reducing the maximum fluence by one-half. This reduction in fluence continues under the overhang until the effective limit for incidence angles is reached. Since the fluence at any point on the etched surface is a summation of atoms for all angles of incidence permitted at that point, it is observed that unshadowed areas receive fluences proportional to the total area under the angular distribution curve (Figure 3), while a partially shadowed surface receives a fluence at each point on the etchable surface that is proportional to the area under the angular distribution curve that is not blocked by the mask. Thus, the etch profile for the half-plane mask is equivalent to plotting the integral of the angular distribution function. The etch profile near a solid step mask (Figure 1c) resembles that for the half-plane mask for the portion in front of the step, but at the step the front face blocks additional fluence resulting in a nearly vertical decrease in the etch depth at the step (approximately 0.1° maximum undercutting relative to a 560 μm mask height occurs for a 9 μm etch depth). The etch profile (Figure 1d) that occurs near a solid knife-edge mask with edges sloped greater than 15° from a normal incidence direction, or near a thin film mask deposited on the etchable surface, is nearly a vertical step.

Scanning electron micrographs, which equally magnify both the horizontal and vertical dimensions, show close range sloped edges even for the etched steps near thin film masks (Figure 4). The close range slopes result from microscopic shadowing by slightly elevated knife edges or by self-shadowing by

the etch steps. With self-shadowing, the height of the step providing the shadowing is continuously increasing with etch depth. The slopes of any etched edges should extend less than 15° relative to the top edge of the shadowing structure for normally incident atoms; thus, the extent of the shadow increases with mask height. A particle, or other contaminant, on the surface would initially mask an area its size, but as etching progresses the shadowed area expands, with most of the fluence shadowing occurring within 7° of the orbital velocity direction and limited essentially to less than 15°. This general profile and limit appears consistent with scanning electron micrographs of etched surfaces (Figure 4). One diffuse etch step (oriented vertically in Figure 4) occurred near a slightly elevated knife edge of an aluminum cover, while another sharp etch step (oriented horizontally in the same figure) occurred at the edge of a niobium thin film pattern deposited on the surface prior to etching. Both steps are similar to the profiles in Figure 1 except the heights of the shadowing structures were small and increased by relatively large amounts with etch depth. Fine microstructures (spiked region in Figure 4) are observed on most etched structures (even amorphous plastics) and are undoubtedly influenced by this self-shadowing effect. It is hypothesized that condensed contaminants, segregated at nucleation sites, or fine particles on the surface provided masking and that self-shadowing created the sloped sides. Accommodation of the fast oxygen atoms may have a lower efficiency at glancing incidence to the surface so further studies are needed to fully test these hypotheses. Similar structures have been observed on ground-based ion-bombarded surfaces [Auciello and Kelly, 1984]. Precleaning has eliminated such structures in semiconductor device fabrications [Wang and Wong, 1983]. Thermal and ensemble velocities, from electrical accelerations in ground-based sputtering plasmas, should create shadowing effects similar to those in orbit.

Actual stylus tracings of some samples flown on STS-8 are shown in Figure 5. One tracing (Figure 5a), which was taken from a vitreous carbon surface that was at the base of a 560-μm-thick solid step, is typical for near alignment of the step with the orbital direction (within 1/2°). Corrections for a chipped edge, an error due to the stylus shank contacting the etch step, and contaminant created peaks are shown by a dashed line (Figure 5a). Other examples where the mask step faces were not aligned with the orbital direction are shown (Figures 2c and 2d), and the excellent steps obtained with niobium thin film masks (Figure 5b) demonstrate the advantages of this type of mask for determining etch rates and reaction efficiencies, especially for rapidly etched materials such as the polycarbonate (CR-39) shown in Figure 5b.

The measured etch profile was digitized and compared to computed etch profiles for different ambient gas temperatures. These were obtained by normalizing the maximum fluence to the maximum etch depth observed and requiring half etch depths to align laterally at zero angle of incidence (Figure 6). This procedure indicated that the average temperature of the oxygen atoms was 750±50 K for the best fit.

Discussion

The range in angular distribution of gas particles incident upon a satellite strongly influences observed degradation effects and the results of numerous measurements. Surfaces facing the forward or "ram" direction are subject to heavy erosion in low Earth orbits if they are combustible and unprotected, while surfaces facing away form the orbital direction ("wake" direction) can experience an ultrahigh vacuum if self-contamination from outgassing and particle scattering is controlled. Such erosion can seriously degrade mechanical and optical surface properties [Peters et al., 1986] or be

used beneficially for cleaning surfaces contaminated with hydrocarbons or other combustible materials. The erosion may also be used as a quantitative sensor of atomic oxygen [Gregory and Peters, 1985]. The usual treatments of equilibrium thermodynamic variables, such as pressure and temperature, have to be modified for observations in orbit. Except for outgassed or accommodated species traveling with the satellite, the orbital velocity dominates relative collision speeds between neutral, thermospheric species, and the orbiting surfaces.

Atoms reflected from the front faces of mask steps could be a source of additional etching, but small cross sections and broad scattering (due to accommodation) appear to reduce this effect below the accuracy of the profile measurements discussed here; however, higher sensitivity reflection measurements of a different nature will soon be reported.

Aligning all etch profiles so they cross at the 50% etch depth was justified on the basis that for symmetrical angular distributions, half of the total fluence is received for angles of incidence on each side of normal incidence; thus, the profiles all pass through 50% etch depth at zero degrees. Nonsymmetrical distributions (nonequilibrium thermally) and large off-normal alignments of surfaces with the orbital velocity direction could require corrections. If the vertical portion of an etch profile associated with a solid step does not occur at the 50% etch depth then the top edge of the step tilts relative to its base (exaggerated in Figures 5c and 5d).
For small tilts the angle can be approximated by arc tangent of horizontal separation between vertical slope and 50% etch divided by the mask height; e.g., arc tangent (12.8/560) = 1.3° is an estimate for Figure 5c. An estimate of 4.5° for Figure 5d seems slightly high and may indicate that a correction is needed. The masking step for Figure 6 was aligned to better than 0.5°.

The theoretical and measured etch profiles matched extremely well considering that the etched surface received a total fluence that was integrated over 41.2 hours with contributions from various latitudes and during day and night conditions. During the STS-8 mission, ambient temperatures varied from approximately 690 K to 1000 K based on extreme conditions and application of mass spectroscopy incoherent scatter (MSIS) and MSFC/J70 thermospheric models (M. Torr and D. Johnson, personal communication, 1986). An estimated average of 826±165 K resulted from the latter model (D. Johnson, unpublished data, 1986).

Summary

Theoretical angular distribution profiles for oxygen atoms incident to surfaces or exiting behind masks have been calculated in an orbiting reference frame. These profiles are dependent upon the ratio of the orbital speed to the most probable thermal speed of the ambient oxygen atoms. The profiles of etched combustible surfaces have been measured and related to such distribution profiles and a temperature of 750±50 K, consistent with the mean ambient temperature at this altitude and for the solar activity during exposure, was obtained. Calculated profiles for a number of mask/substrate configurations were given.

References

Auciello, O., and R. Kelly, (Eds.), Ion Bombardment Modification of Surfaces, 466 pp.,Elsevier, New York, 1984.

Gregory, J. C., and P. N. Peters, Interaction of atomic oxygen with solid surfaces at orbital altitudes (A0114), in The long Duration Exposure Facility (LDEF), NASA SP-473, edited by L. G. Clark et al., pp. 14-18, 1984.

Gregory, J. C., and P. N. Peters, The production of glow precursors by oxidative erosion of spacecraft surfaces, in Second Workshop on Spacecraft Glow, NASA CP-2391, edited by J. H. Waite, Jr., and T. W. Moorehead, pp. 174-179, 1985.

Leger, L. J., Oxygen atomic reaction with shuttle materials at orbital altitudes, NASA TM-58246, May 1982.

Nocilla, S., The surface re-emission law in free molecule flow, in Rarified Gas Dynamics, edited by J. A. Laurmann, pp. 327-346, Academic Press, New York, 1963.

Peters, P. N., R. C. Linton, and E. R. Miller, Results of apparent atomic oxygen reactions on Ag, C, and Os exposed during the Shuttle STS-4 orbits, Geophys. Res. Lett., 10, 569-571, 1983.

Peters, P. N., J. C. Gregory, and J. T. Swann, Effects on optical systems from interactions with oxygen atoms in low Earth orbits, Applied Optics, 25, 1290-1298, 1986.

Visentine, J. T., L. J. Leger, J. F. Kuminecz, and I. K. Spiker, STS-8 Atomic oxygen experiment, AIAA Paper No. 85-0415, 1985.

Wang, D., and J. Wong, Etched trenches conserve semiconductor device space, Res. & Dev., 27, 107-112, 1983.

Figure Captions

Figure 1. Theoretical etch profiles (lower cross sections) for several masking configurations (shown schematically on top). The lower cross sections are greatly magnified vertically as occurs in stylus profilometry measurements.

Figure 2. Calculated angular distributions for atoms (orbital velocity along the 0-180 axis) for three orbital to most probable thermal speed ratios.

Figure 3. Rectangular plot of the angular distributions (a) during high solar activity (T ≈ 1300 K) and solar minimum (T ≈ 600 K) conditions. The integral of these distributions (b) relates to the etch profiles.

Figure 4. Scanning electron micrograph of an etched CR-39 plastic surface showing edge profiles where a knife-edged cover was located and where a Nb thin film is still located (photographed by A. Dorries).

Figure 5. Stylus profilometry tracings taken from samples flown on STS-8. Profiles (a), (c), and (d) are from etched vitreous carbon near solid step masks, and (b) is from a polycarbonate plastic surface on which a niobium thin film pattern was deposited.

Figure 6. Comparison of a measured etch profile (partially corrected for: chipped edge, contaminants, and stylus shank contacting step edge) with the theoretical profiles for 600 K and 1300 K ambient temperatures. Best fit to measured profile occurs for 750±50 K.

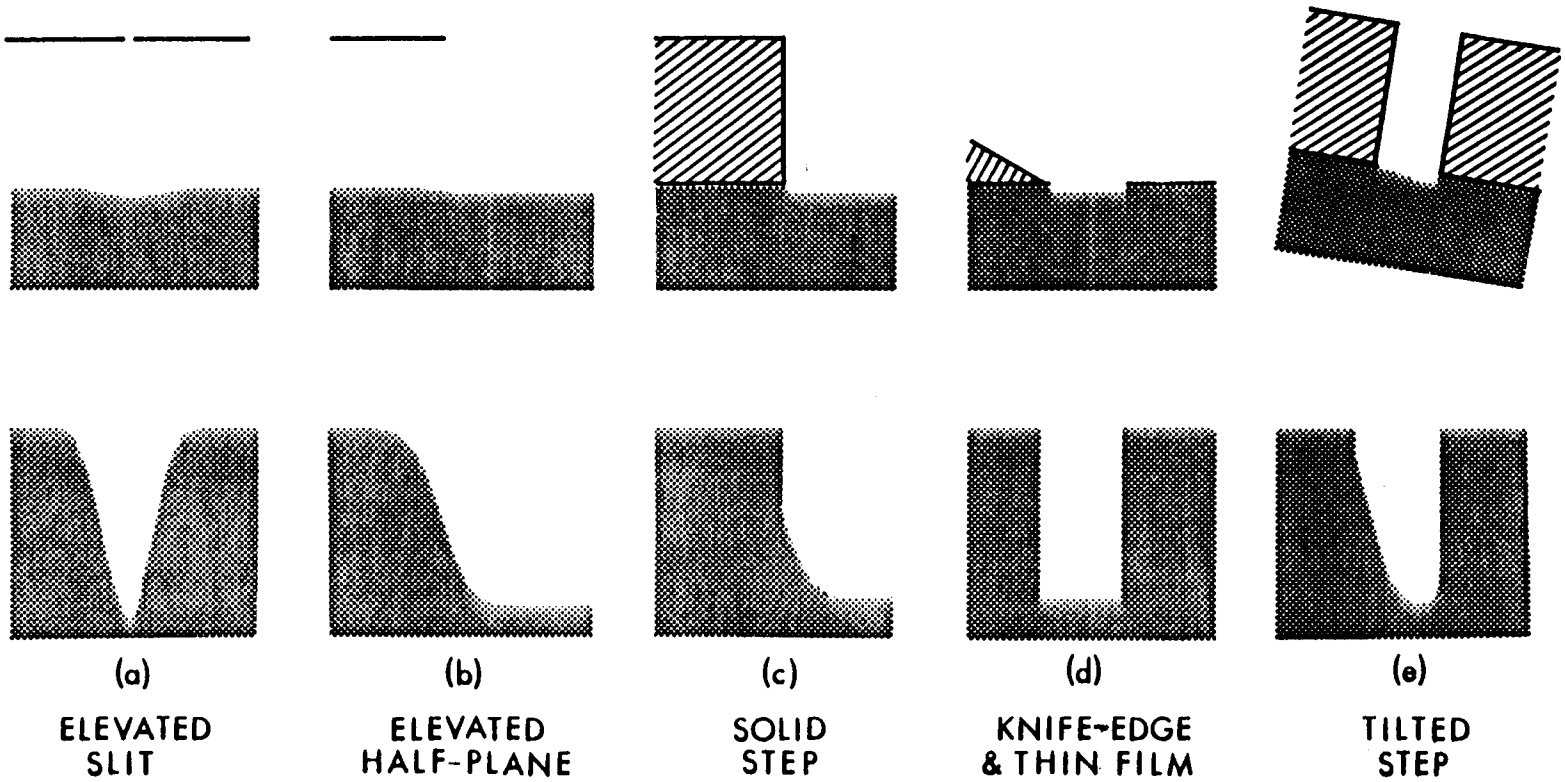
(a)
ELEVATED SLIT
(b)
ELEVATED HALF-PLANE
(c)
SOLID STEP
(d)
KNIFE-EDGE & THIN FILM
(e)
TILTED STEP

Fig. 1

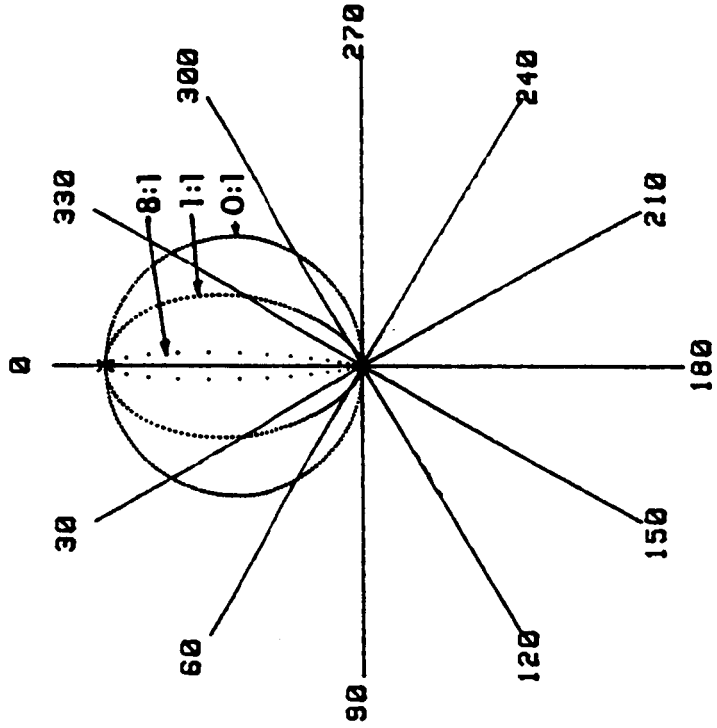

Fig. 2

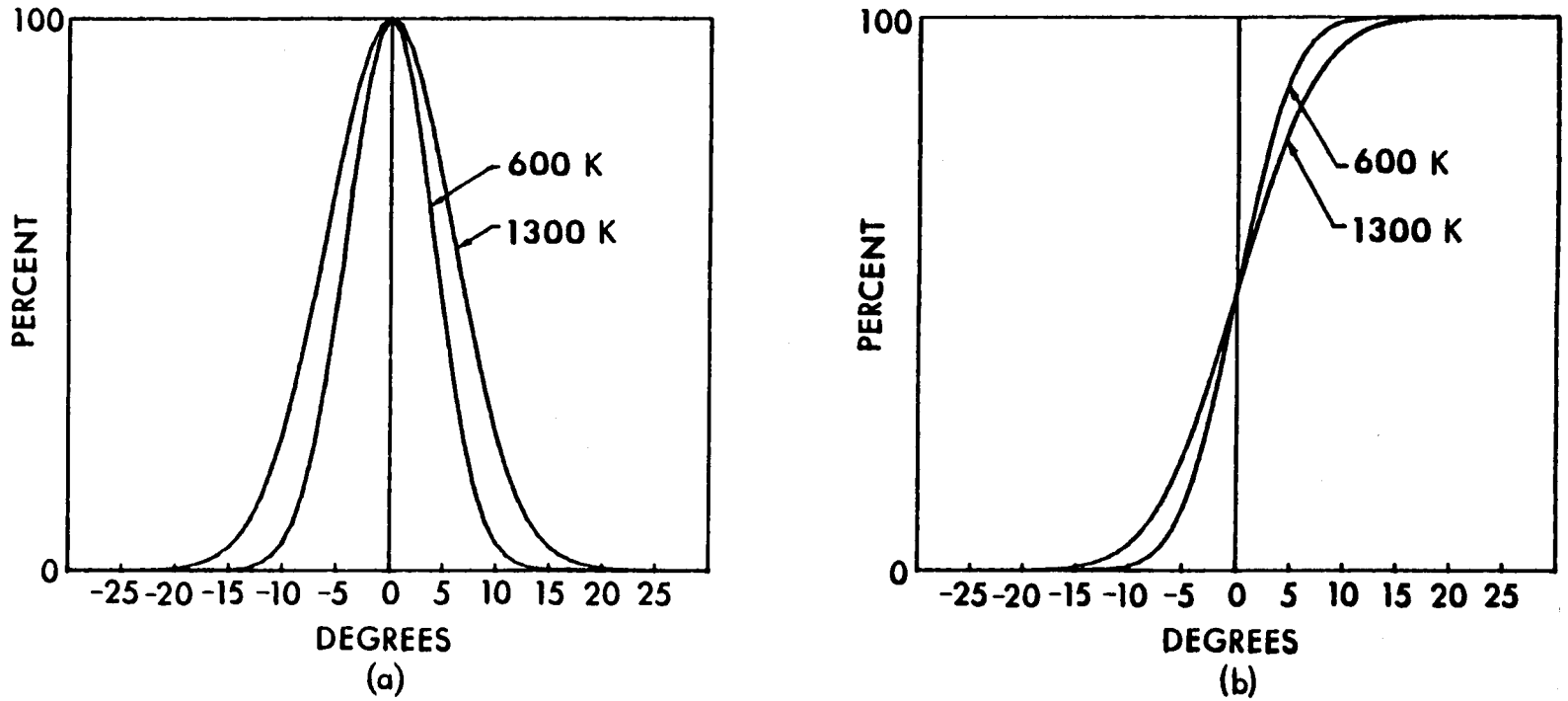
100
0
PERCENT
600 K
1300 K
-25 -20 -15 -10 -5 0 5 10 15 20 25
DEGREES
(a)
100
0
PERCENT
600 K
1300 K
-25 -20 -15 -10 -5 0 5 10 15 20 25
DEGREES
(b)

Fig. 3

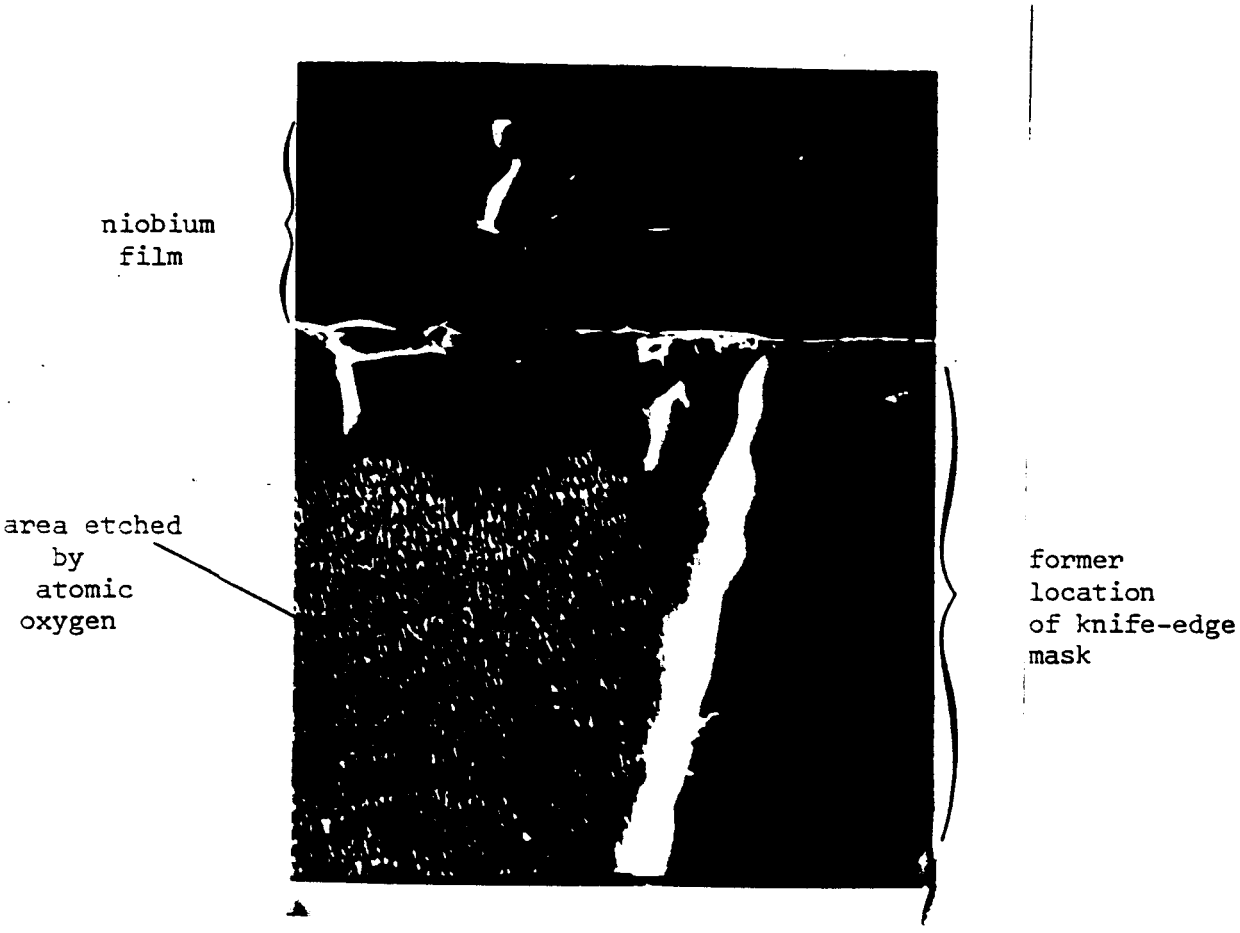
niobium
film
area etched
by
atomic
oxygen
former
location
of knife-edge
mask

Fig. 4

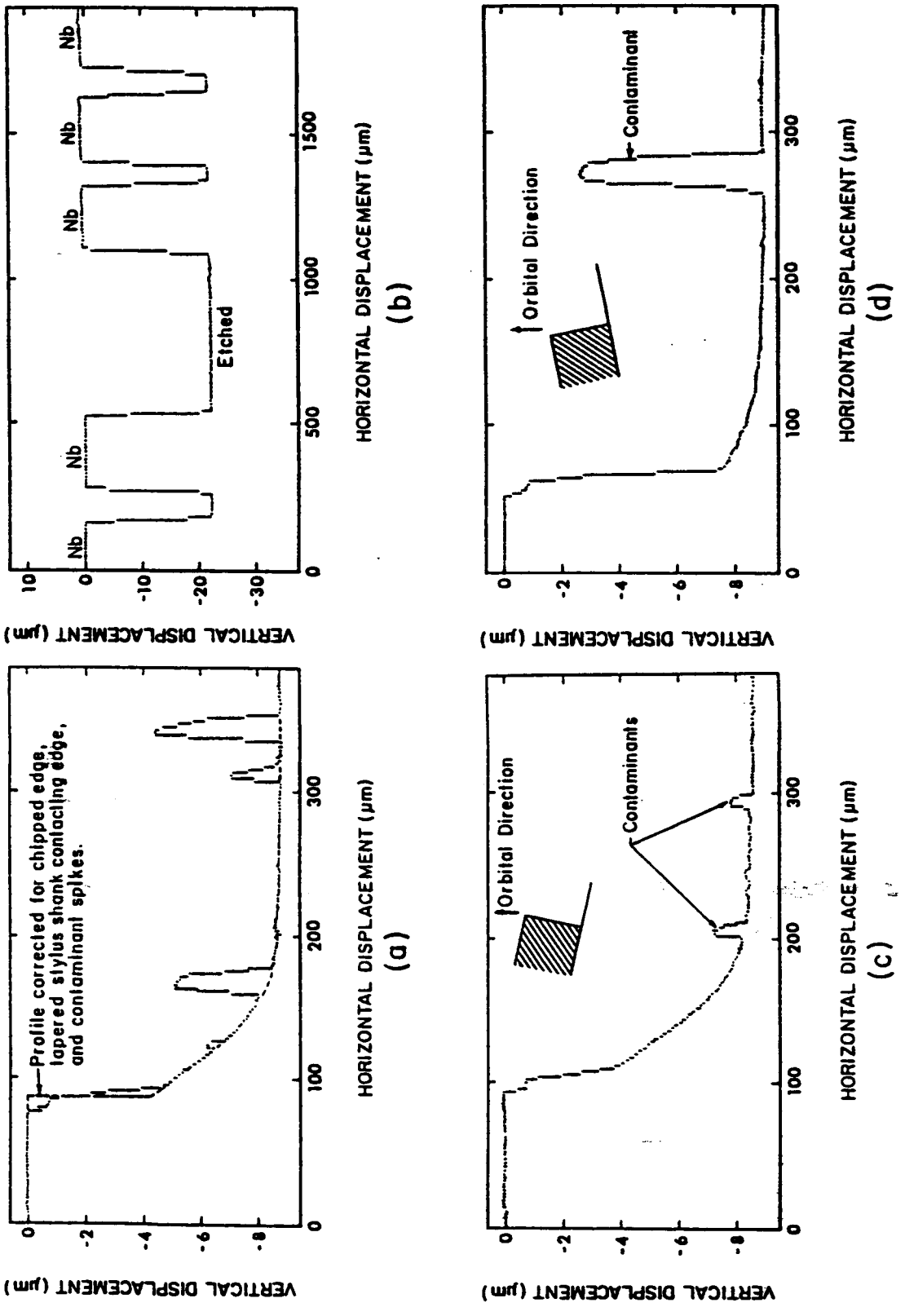
Nb
Nb
Nb
Nb
Nb
Etched
VERTICAL DISPLACEMENT (μm)
HORIZONTAL DISPLACEMENT (μm)
(b)
Profile corrected for chipped edge, tapered stylus shank contacting edge, and contaminant spikes.
(a)
Orbital Direction
Contaminant
(d)
Orbital Direction
Contaminants
(c)

Fig. 5

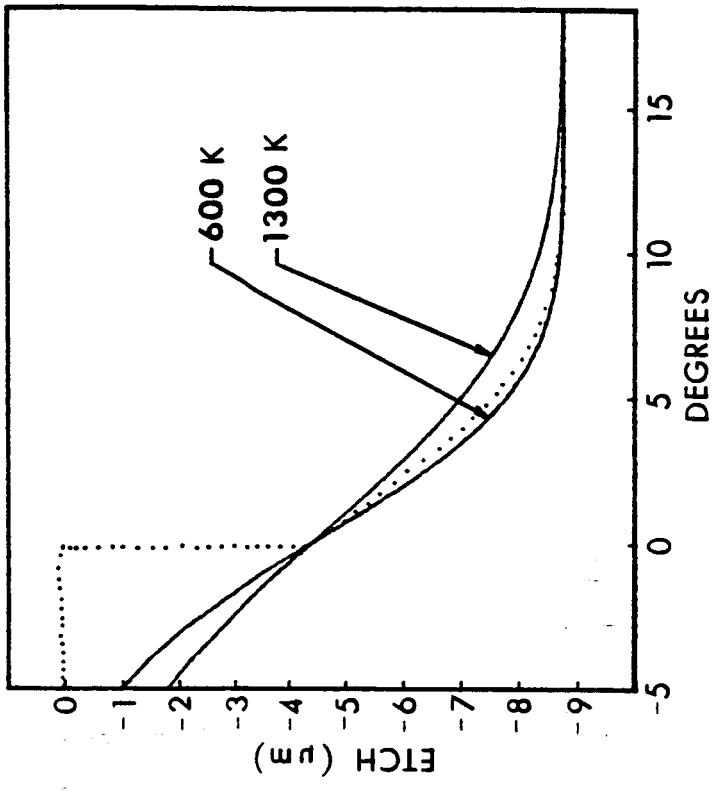

Fig. 6